University of Baghdad
College of Engineering
JOURNAL OF ENGINEERING

Journal of Engineering

journal homepage: www.jcoeng.edu.iq
Number 3 Volume 24 Month 3

Mechanical and Energy Engineering

Numerical Investigation of the Effect of Inserted Twisted Tape inside Submerged Bundle Tubes on its Thermal Performance

Dr. Kamal Mohammed Ali
Umarah Institute of Technology
Southern Technical University
al_ssafar2005@yahoo.com

Abdalrazzaq K. Abbas
Department of Mechanical Engineering
College of Engineering, University of Kerbala, Iraq
abd_abbas1967@yahoo.com

ABSTRUCT

Twisted tape insertion in smooth plain tube is one of types of passive methods that is used to enhance heat transfer. Swirl fluid flow inside tube and related heat transfer characteristics are very complex. ANSYS FLUENT (V 16.1) and ASPEN industrial program are used in analyzing this technique for enhancement heat transfer. A circular plain tube has length L=8534mm and 17 mm inner diameter with twisted tape has twist ratio of y = (H/D) = (150/17) =8.8 along with a plain tube were considered for this study. Eight Reynolds numbers (Re) of 784, 1000, 2000, 3000, 4000, 5000, 6000 and 7000 are used to analyze the response of thermal performance. Crude oil API 28 exit temperature, film heat transfer coefficient, Nusselt number and overall enhancement ratio results are presented for both empty and inserted plain tube with comparison between the two cases. An increase of 0.76 to 2.36 overall enhancement is predicted with twist ratio 8.8 for Reynolds number 784 to 7000 respectively.

Keywords: Heat transfer enhancement, friction factor, twist ratio, heat exchanger, twisted tape, laminar and turbulent flow.

التحقق عدديا لتأثيرات الشريط الملتوي المدخل داخل أنابيب الحزمة المغمورة على أدائها الحراري

د. كمال محمد علي
المعهد التقني / العمارة
الجامعة التقنية الجنوبية

عبد الرزاق خضير عباس
قسم الميكانيك - كلية الهندسة – جامعة كربلاء

الخلاصة

الشريط الملتوي المدخل داخل الانبوب ذو السطح العدل هو أحد الطرق الغير مستهلكة لطاقة خارجية المستخدمة لتحسين انتقال الحرارة. الجريان الحلزوني للمائع داخل الانبوب وخصائص انتقال الحرارة المصاحبة هي معقدة جدا. ANSYS FLUENT (V 16.1) والبرنامج الصناعيASPEN استخدمت لتحليل هذا الأسلوب في تحسين انتقال الحرارة. الانبوب الدائري ذو السطح العدل هو بطول 8534 ملمتر وقطر داخلي 17ملمتر ونسبة التواء (150/17) =8.8 على طول الانبوب اعتمد في هذه الدراسة. ثمان أرقام لرينولدز (784, 1000, 2000, 3000, 4000, 5000, 6000, 7000) استخدمت لفحص تاثر الاداء الحراري. درجة حرارة خروج النفط الخام API28 ومعامل انتقال الحرارة ورقم Nusselt والنسبة الكلية للتحسين قدمت لكل من الانبوب ذو السطح العدل الفارغ وللذي يحتوي على شريط الملتوي مع المقارنة بين الحالتين. أزدياد 0.67 الى 2.36 في التحسين الكلي قد وجد مع نسبة التواء 8.8 لارقام Reynolds 784 الى 7000 على التوالي.

مفتاح الكلمات: تحسين انتقال الحرارة ، عامل الاحتكاك، نسبة الالتواء ، مبادل حراري , الشريط الملتوي، جريان طباقي ومضطرب.

1. INTRODUCTION

Crude oil in order to be suitable for export, gases must be removed from it through special equipment and then need to be warming from 30ºC to 70ºC which is the suitable degree for desalter process which was done in special equipment. Heated process of crude oil was done in tube bundle submerged in a large shell, full of water at 95ºC to 98ºC, where the water in shell heated by burners operated at the fuel gases that was separated and removed from the crude oil previously. Hundreds of tubes were in tubes bundle. Therefore, it is economic to reduce number of tubes in the bundle with keeping the same amount of heat transfer to the crude oil inside tubes through the enhancement heat transfer process.

Several methods of heat transfer enhancement were used to increase heat transfer with keeping same performance of overall system. Passive and active methods were utilized as techniques of enhancing heat transfer. Passive methods don't need an external power antithesis to the active methods. Insertion of twisted tape is one of the most effective passive techniques as shown **Fig. 1.** Twisted tape produce swirl and turbulence, which are important to boost heat transfer. It increases the flow path length and so more residence time, thus the heat transfer is improved and greater frictional losses. So that, in this study, inserted twisted tape was used to enhance the heat transfer coefficient inside tubes that flow in it crude oil API 28.

Eiams-aard, et al., 2006, studied the heat transfer and friction factor characteristics in a double pipe heat exchanger where the inner pipe was inserted with equally spaced elements of twisted tape. The heat transfer coefficient was proportional directly with twist ratio, whereas the increase in the free space ratio, improves both the heat transfer coefficient and friction factor. **Woei Chang, et al., 2007,** studied experimentally the increase of heat transfer inside a tube inserted with serrated twisted tape for several twist ratios. The augmentation of heat transfer with inserted serrated twisted tape was 1.25–1.67 times than with the plain twisted tape. **Woei Chang, et al., 2007,** studied experimentally the heat transfer coefficients and axial pressure drop of the tube inserted with a broken twisted tape of twist ratio 1, 1.5, 2, 2.5 and 1 was performed in the Re range of 1000–40,000.. Mean Fanning friction factors and local Nusselt numbers were proportional inversely with the twist ratio. Thermal performance factors, mean Fanning friction factors and Heat transfer coefficients in the tube fitted with the broken twisted tape are, respectively, augmented to 0.99–1.8, 2–4.7, 1.28–2.4 times of those in the tube fitted with the smooth twisted tape. Empirical pressure drop and heat transfer correlations which evaluate the mean Fanning friction factor and local Nusselt number for the tube with the broken twisted tape insert were generated. **Bharadwaj, et al., 2009,** studied experimentally the pressure drop and heat transfer characteristics of water flow in smooth tube and spirally grooved tube inserted with twisted tape and compared between them. In the laminar flow, spirally grooved tube without twisted tape has more increase in heat transfer than with twisted tape insert. **Eiamsa-ard** and **Promvonge, 2010,** experimentally studied arrangement effect of alternate clockwise and counterclockwise rotation of twisted tape inserts inside circular tube on heat transfer enhancement. It was found that the heat transfer rate was more than one with typical twisted tape insert. **Naga Sarada, et al., 2010,** investigated experimentally heat transfer of turbulent flow in a horizontal tube with twisted tape of varying width. The enhancement of heat transfers with twisted tape inserts varied from 36% to 48% as compared to plain tube for full width inserts. **Thianpong, et al., 2011,** investigated experimentally the effects of plain and perforated twisted tape inside circular tube on heat transfer enhancement. It was found that tubes with perforated twisted tape and plain twisted tape yielded heat transfer enhancement up to 208% and 190% over plain tube, respectively. **Murugesan, et al., 2011,** investigated experimentally the effect of V-cut

twisted tape inserted inside tube. Mean friction factor and mean Nusselt number increase with increasing depth ratios (depths of V cut / tape width) and decreasing of width ratios and twist ratios. **Bas** and **Ozceyhan, 2012,** investigated experimentally the effect of clearance ratio (clearance/ tube diameter) and twist ratio of twisted tape inserted inside tube on flow friction and heat transfer behavior. It was found that the heat transfer rate was proportional inversely with clearance ratio. **Gunes, et al., 2012,** investigated numerically pressure drop and heat transfer inside a tube fitted with equally spaced elements of twisted tape having different tape width. Within a range of Reynolds number, the effects of twisted tape width and space ratio on the heat transfer and friction characteristic was reported. **Giniyatullin**, **et al., 2014,** studied experimentally Nusselt number and friction factor data for laminar flow of viscous oil inside spiral corrugation tube and fitted with twisted tape with oblique teeth. The twisted tape with oblique teeth in spiral corrugation tube implemented better enhancement technique than the individual techniques. **Ramakumar, et al., 2016,** investigated numerically the performance of tapered twisted tape inserted inside a circular plain tube for three Reynolds numbers of 8545, 11393, and 13333 with taper angles of 0.3, 0.4, 0.5, 0.6, and 0.7 and a twist ratio of 3 via ANSYS FLUENT v14.0. Pressure drop and heat transfer data were presented in the form of friction factor, Nusselt number, and overall enhancement ratio. It was found an increase of 17% in overall enhancement with 0.5 taper angle over conventional tape. **Yang, et al., 2016**, presented a mathematical model for smooth (ST) and corrugated (CT) tubes inserted with twisted tape at twisted ratio 2.5. The heat transfer enhancements and friction loss behaviors was numerically investigated. RNG k-ε turbulence model was applied. Comparisons between CT and ST were done, where ($Nu_{corrugated}/Nu_{smooth}$) ratio was 1.36.

From above, a good number of researchers focused on heat transfer enhancement and fluid friction behaviors inside circular tube fitted with twisted tape. The centrifugal forces generated by twisted tape produce swirling fluid flow which that boosts the heat transfer rate with penalty on pressure loss. The present study aims to analyze numerically a propose twisted tape with twisted ratio 8.8 inside plain tube for different Reynolds number with operational performance comparison between tube inserted with twisted tape and empty plain tube. The difference between this work and other survived researches can be listed in these points:

- Simulate actual process case in the refinery plant (tube length, tube diameter, fluid flow-API 28, twisted ratio, range of Reynolds numbers, inlet pressure, inlet temperature and mass flow rate).
- Using Aspen industrial program to do the comparison with ANSYS fluent simulation for this case study, where Aspen is normally used by Americans oil refineries companies for designing refinery equipment, so that this comparison can indicate the close amount between CFD and Aspen industrial program which represent the reference for manufacturing companies.
- No work was found in the surveys doing the upper two points.

2. NUMERICAL METHOD AND PROBLEM FORMULATION

A three-dimensional steady state system of laminar and turbulent flow in a plain tube has length L=8534mm and 17 mm inner diameter equipped with a twisted tape has a twist ratio y = (H/D) = (150/17) =8.8 along the tube is considered in the present study. The physical model simulates the flow of crude oil API 28 in a heat exchanger tubes. Heat added to the outer tube walls via hot water where the heat transfers through the tube wall by conduction and to crude oil inside tube via convection.

2.1 Numerical Solution

In order to mathematically analyze the heat transfer characteristics of heat exchanger fluid flow in plain empty and inserted plain tube, a Navier-Stokes equation solution is required. Due to the complexity of twisted surface configuration and the significant viscous and heat effects, a numerical technique using the solver ANSYS-FLUENT version 16.1 which uses the finite-volume method to solve the governing equations through using a pressure-based solver. Two turbulence model, $v^2 - f$ and k-ε are used to solve governing partial differential equations of mass, momentum and energy conservations in three dimensions. A $v^2 - f$ turbulence model involves solution of the four transport equations; turbulence kinetic energy k, its rate of dissipation ϵ, velocity variance scale $\bar{v}^2$ and elliptic relaxation function f, to demonstrate the effect of the turbulence on the flow structure.

2.1.1 Mesh

Pointwise V17.0R1 is used to generate structured, unstructured and hybrid grids. Structured grid is used for tube surface while unstructured grid is used for flow cross section which result a hybrid mesh in the block that a mixture from hexahedron, pyramid and prism cells as, shown in **Fig. 2**. A fine mesh is created on the flow cross section to resolve the thermal boundary layer.

The solution to be accurate in this work, skewness kept up to 0.85 for hex, quad and triangular cells and up to 0.9 for tetragonal cells. For structured domains the orthogonality of grid points adjacent to the tube wall is kept to perfect orthogonality and max value 90° along the entire tube surface. For the present twisted model 5,769,257 cells are used while for empty tube model 4,941,189 cells uses. The rate of convergence is an indication to mesh quality. In this work the convergence is achieved with about 500 iterations.

2.1.2 Governing Equation and Assumptions

The numerical study of this work depends on the actual crude oil heat exchanger conditions that is specified and is used in crude oil transport plant. Crude oil conditions are represented by density 865 kg/m³, specific heat 1982J/kg. K, thermal conductivity 0.129 W/m.K and viscosity 0.00752kg/m. s at Reynolds number 784. Other values of Reynolds number are studied to predict the effect of Re on the thermal performance. This research will focus on the effect of inserted twisted tape in plain tube on crude oil heat exchanger thermal performance for ranges of Reynolds number 784, 1000, 2000, 3000, 4000, 5000, 6000, and 7000 for crude oil API 28 flow.

The characteristic Reynolds number depends on tube hydraulic diameter which equal to inner tube diameter as a characteristic length and 5% turbulent intensity at free stream inlet velocity is used.

In the present study, crude oil API 28 is a fluid inside tube. The flow characteristics are assumed to be as follows:

1- Three-dimensional.
2- Incompressible flow, Ma<0.3.
3- Density ρ varies only with temperature.
4- Laminar and turbulent flow.
5- Steady state flow in main flow.
6- Newtonian fluid.
7- Single-phase flow.
8- Flows pressure work $\frac{P}{\rho}$, and kinetic energy $\frac{V^2}{2}$ terms in energy equation are negligible.

9- Viscous dissipation terms $\left(\bar{\bar{\tau}}_{eff}.\vec{V}\right)$ are negligible.
10- Chemical reaction heat $S_h = 0$.
11- Fully developed flow.

The following governing equations were solved for laminar flow using ANSYS Fluent solver:
Mass conservation

$$\nabla.(\rho u) = 0 \quad (1)$$

Momentum conservation
X-momentum equation

$$\rho\left(u\frac{\partial u}{\partial x} + v\frac{\partial u}{\partial y} + w\frac{\partial u}{\partial z}\right) = -\frac{\partial p}{\partial x} + \mu\left(\frac{\partial^2 u}{\partial x^2} + \frac{\partial^2 u}{\partial y^2} + \frac{\partial^2 u}{\partial z^2}\right) \quad (2)$$

Y-momentum equation

$$\rho\left(u\frac{\partial v}{\partial x} + v\frac{\partial v}{\partial y} + w\frac{\partial v}{\partial z}\right) = -\frac{\partial p}{\partial x} + \mu\left(\frac{\partial^2 v}{\partial x^2} + \frac{\partial^2 v}{\partial y^2} + \frac{\partial^2 v}{\partial z^2}\right) \quad (3)$$

Z-momentum equation

$$\rho\left(u\frac{\partial w}{\partial x} + v\frac{\partial w}{\partial y} + w\frac{\partial w}{\partial z}\right) = -\frac{\partial p}{\partial x} + \mu\left(\frac{\partial^2 w}{\partial x^2} + \frac{\partial^2 w}{\partial y^2} + \frac{\partial^2 w}{\partial z^2}\right) \quad (4)$$

The following governing equations were solved for Turbulent flow using ANSYS Fluent solver:
In this work Reynolds averaged Navier-Stokes equations RANS are used.
In Cartesian tensor, they can be written as:

$$\frac{\partial \rho\bar{u}_i}{\partial x_i} = 0 \quad (5)$$

$$\frac{\partial}{\partial x_j}\rho\bar{u}_i\bar{u}_j = -\frac{\partial \bar{P}}{\partial x_i} + \frac{\partial}{\partial x_j}\left[\mu\left(\frac{\partial \bar{u}_i}{\partial x_j} + \frac{\partial \bar{u}_j}{\partial x_i} - \frac{2}{3}\delta_{ij}\frac{\partial \bar{u}_i}{\partial x_i}\right)\right] + \frac{\partial}{\partial x_j}\left(-\rho\overline{\acute{u}_i\acute{u}_j}\right) \quad (6)$$

where $\left(-\rho\overline{\acute{u}_i\acute{u}_j}\right)$ is a Reynolds stress tensor R_{ij} which represents the effects of turbulence. The form of energy equation that is solved in ANSYS FLUENT was:

$$\nabla.\vec{V}\rho E + P = \nabla.\left(k_{eff}\nabla T - \sum_j h_j\vec{J}_j\right) \quad (7)$$

ANSYS theory guide, 2014.

2.1.3 $v^2 - f$ Turbulence Model

The flow inside tube is a boundary layer flow. The most suitable turbulent model for fluid flow inside empty plain tube considering the boundary layer is $v^2 - f$ model. The turbulence kinetic energy k, rate of dissipation ε, the velocity variance scale $\overline{\acute{v}^2}$, and the elliptic relaxation function f can be obtained from the following transport equations:

$$\frac{\partial}{\partial x_i}(\rho k\bar{u}_i) = P_k - \rho\varepsilon + \frac{\partial}{\partial x_j}\left[\left(\mu + \frac{\mu_t}{\sigma_k}\right)\frac{\partial k}{\partial x_j}\right] \quad (8)$$

$$\frac{\partial}{\partial x_i}(\rho\varepsilon\bar{u}_i) = \frac{\acute{C}_{\varepsilon 1}P_k - C_{\varepsilon 2}\rho\epsilon}{T} + \frac{\partial}{\partial x_j}\left[\left(\mu + \frac{\mu_t}{\sigma_\varepsilon}\right)\frac{\partial \varepsilon}{\partial x_j}\right] \quad (9)$$

$$\frac{\partial}{\partial x_i}\left(\rho\overline{\acute{v}^2}\bar{u}_i\right) = \rho k f - 6\rho\overline{\acute{v}^2}\frac{\varepsilon}{k} + \frac{\partial}{\partial x_j}\left[\left(\mu + \frac{\mu_t}{\sigma_k}\right)\frac{\partial\overline{\acute{v}^2}}{\partial x_j}\right] \quad (10)$$

$$f - L^2\frac{\partial^2 f}{\partial {x_j}^2} = (C_1 - 1)\frac{\frac{2}{3} - \frac{\overline{\acute{v}^2}}{k}}{T} + C_2\frac{P_k}{\rho k} + \frac{\frac{5\overline{\acute{v}^2}}{k}}{T} \quad (11)$$

The model constants have the following default values:
$\alpha = 0.6$, $C_1 = 1.4$, $C_2 = 0.3$, $C_{\varepsilon 1} = 1.4$, $C_{\varepsilon 2} = 1.9$, $(C_\eta = 70)$, $C_\mu = 0.22$, $C_L = 0.23$, $\sigma_k = 1$, $\sigma_L = 1.3$, $\acute{C}_{\varepsilon 1} = C_{\varepsilon 1}\left(1 + 0.045\sqrt{k/\overline{\acute{v}^2}}\right)$, **ANSYS Fluent $v^2 - f$ turbulence model manual, 2013.**

2.1.4 Transport Equations for the RNG k-ε Model

Mathematical technique called "renormalization group" (RNG) methods is used to model the RNG-based *k-ε* turbulence model that is derived from the instantaneous Navier-Stokes equations. RNG *k-ε* turbulence model with enhanced wall treatments is used to model the case study with effective accounts of viscosity for Low-Reynolds number. The effect of swirl on turbulence is included in the RNG model.

The *k* and *ε* equations are:

$$\frac{\partial}{\partial x_i}(\rho k u_i) = \frac{\partial}{\partial x_j}\left(\alpha_k\,\mu_{eff}\frac{\partial k}{\partial x_j}\right) + G_k + G_b - \rho\varepsilon - Y_M + S_K \quad (12)$$

$$\frac{\partial}{\partial x_i}(\rho\varepsilon u_i) = \frac{\partial}{\partial x_j}\left(\alpha_\varepsilon\mu_{eff}\frac{\partial\varepsilon}{\partial x_j}\right) + C_{1\varepsilon}\frac{\varepsilon}{k}(G_k + C_{3\varepsilon}G_b) - C_{2\varepsilon}\rho\frac{\varepsilon^2}{k} - R_\varepsilon + S_\varepsilon \quad (13)$$

The term G_k represents the generation of turbulence kinetic energy due to the mean velocity gradients. G_b is the generation of turbulence kinetic energy due to buoyancy. Y_M represents the contribution of the fluctuating dilatation in compressible turbulence to the overall dissipation rate. The quantities α_k and α_ε are the inverse effective Prandtl numbers for k and ε, respectively. S_k and S_ε are user-defined source terms. Hence, for the present study, the turbulent flow is modeled using the k-ε viscous turbulence model with turbulent coefficients $C\mu$=0.0845, $C_1\varepsilon$ =1.42, $C_2\varepsilon$=1.68, S_k =Sε =0, $\alpha_k = \alpha_\varepsilon$ =1.393. Semi implicit pressure linked equation method (SIMPLE) is used for pressure velocity coupling.

The second-order upwind discretization scheme is used for turbulence kinetic energy and dissipation. The second-order discretization scheme is used for momentum and energy equations. The convergence criterion of 10^{-6} is chosen in addition to the selected monitored properties.

2.2 Boundary Conditions and Assumptions

Boundary conditions are specified for each zone of the computation domain. For the steady state, there are three boundary conditions in the physical flow domain, inlet, outlet and solid surfaces wall as shown in figure 2. However, the internal domain zone that shares common areas faces does not require any boundary condition.
The boundary conditions that are used in this work are as follow:

- Inlet temperature $T_\infty = 313$k.

- Inlet and outlet turbulent intensity $T_u = 5\%$.
- Hydraulic diameter D_h =17mm.
- Inlet pressure gage=0.
- No-slip and constant tube wall temperature at 370K.
- No-slip and zero heat flux at the wall of twisted tape.
- Zero-gradient boundary condition for the variable f (elliptic relaxation function) at inlets with default value $= 1$
- The direction of the flow was defined to be normal to the inlet boundary.
- k, ε , $\overline{v^{\prime 2}}$ and ℓ at inlet boundaries were compute its initial values from:

  $k = 1.5(T_u \mathrm{U}_\infty)^2$; $\varepsilon = 0.09^{0.75}\frac{k^{3/2}}{\ell}$; $\overline{v^{\prime 2}} = \frac{2}{3}k$; $\ell = 0.07(D_h)$,

  ANSYS Fluent $v^2 - f$ turbulence model manual, 2013.

And the assumptions are:

- The wall of the tube was assumed to be perfectly smooth with zero roughness.
- Heat conduction in the twisted tape is neglected.

2.3 Data Reduction

From the simulation, the heat transfer rate of the entire tube wall (Q) is obtained for constant temperature boundary condition. Wall heat flux, Nusselt number, friction factor, and overall enhancement ratio are calculated by the equations

$$q = \frac{Q}{A} \quad (14)$$

where the surface area A is given by

$$A = \pi D L \quad (15)$$

The convective heat transfer coefficient is calculated from

$$h = \frac{q}{(T_s - T_{avg})} \quad (16)$$

where T_s was pipe wall temperature and T_b is bulk temperature calculated from

$$T_{avg} = \frac{(T_i + T_o)}{2} \quad (17)$$

The Nusselt number is calculated from

$$N_u = \frac{hD}{k} \quad (18)$$

The friction factor is determined from the pressure drop across the pipe

$$4f = \frac{\Delta P}{\left\{\left(\frac{L}{D}\right)\left(\frac{\rho U^2}{2}\right)\right\}} \quad (19)$$

The overall enhancement ratio is calculated from

$$\eta = \frac{\left(\frac{N_u}{N_{u_P}}\right)}{\left(\frac{f}{f_p}\right)^{1/3}} \quad (20)$$

3. RESULTS AND DISCUSSION

The use of twisted tape inside tube leads to increase in pressure drop and heat transfer over plain tube. From simulation results, the preferable operating system of twisted tape element is found at low Reynolds number where that leads to more compact heat exchanger. The laminar model is considered for Reynolds number up to 2000 while $v^2 - f$ and *k-ε* turbulence models are used to solve the governing equations for Reynolds number above 2000. The converge simulation values of flow inside plain tube inserted with twisted tape for flow above Reynolds number 2000 is obtained with the *k-ε* turbulence model, while the converge simulation values of flow inside plain empty tube is found with $v^2 - f$ turbulence model. Thus, all values above Reynolds 2000 in figures of this work is obtained from using $v^2 - f$ turbulence model for flow in empty plain tube and *k-ε* for flow in plain tube inserted with twisted tape.

Figure 3 clarifies bulk exit temperature of crude oil API 28 from empty plain tube and plain tube with inserted twisted tape. For plain empty tube, it is clear that the results of bulk exit temperatures that are calculated from ANSYS- Fluent and Aspen industrial program are very close, where for laminar flow only 0.3% to 0.8% temperature difference for Reynolds number up to 3000 respectively while for turbulent flow the temperature difference was 0.9% to 1.8% for Reynolds number 4000 to 7000 respectively. The reason of this close in laminar flow was related to the coincidence between Aspen analytical and CFD solutions. These small differences between Aspen analytical and CFD solutions related to CFD model mesh cells numbers. While the close in turbulent flow related to the good agreement between Aspen correlations and $v^2 - f$ CFD method which is the accurate turbulent model to solve turbulent flow near the wall that is generated from increasing flow Reynolds number in plain empty tube, (not from turbulators).

For plain tube inserted with twisted tape, the percentage difference in bulk exit temperature that is calculated from ANSYS-Fluent and Aspen industrial program are 3.7% to 0.29% for Reynolds number 784 to 2000 respectively, while the difference is less than 1% when using *k-ε* turbulence model, and 0% to 3.6% when using $v^2 - f$ turbulence model for Re ≥ 3000. In the actual process, the Aspen industrial program is very close to actual plant data and it is widely used by American manufacturing companies that are specialize in manufacturing processes equipment. Since the results from *k-ε* turbulence model are very close to Aspen industrial program than $v^2 - f$ turbulence model for flow inside empty tube inserted with twisted tape, thus, *k-ε* turbulence model is more accurate than $v^2 - f$ model for simulated swirling flow inside tube, and the reason of that is related to that the *k-ε* model equation contains swirling flow parameter, while $v^2 - f$ turbulence model is accurate for flow inside empty plain tube (flow without swirling) rather than *k-ε* model which the solve diverging in it.

It is clear from **Fig. 4** that the static pressure difference between inlet and outlet boundary for plain tube inserted with twisted tape is higher than static pressure difference for empty plain tube due to the increase in surface frication area that is generated from twisted tape walls and the increase in length flow bath and this difference increase with increasing of flow Reynolds numbers. As shown in **Fig. 5** the percentage increase of static pressure difference(%ΔP) between inlet and outlet tube boundaries are 141%, 137%, 329%, 197%, 176%, 171%, 160% and 146% above that for empty plain tube for Reynolds numbers 784, 1000, 2000, 3000, 4000, 5000, 6000 and 7000 respectively. It is clear that the higher static pressure difference percentage increase is

happened at Re=2000 because the changing the behavior of flow from laminar to turbulent, so it's favorite to a void flow at Re=2000. The friction factor at inner surface tube wall for plain tube inserted with twisted tape is higher than of empty plain tube as shown in **Fig. 6**, which has the same percentage increases of **Fig. 5** due to the relation between them related to equation 19.

As shown in **Fig. 7,** the average Nusselt number of flow inside empty plain tube is increased slowly in laminar flow Re ≤ 2000 and then jumping in average Nusselt number is happened as Reynolds number are increased above 2000 with slowly increasing with Reynolds number increasing. The reason of this jumping is related to the converted of flow from laminar to turbulent, while the behavior of average Nusselt number of flow inside tube inserted with twisted tube is increasing continuously in straightway for Reynolds up to 7000. For laminar flow, the twisted tape is generated swirling to the flow which leads that most of laminar flow path lines is passed through the film heat transfer zone, while for turbulent flow it makes good turbulent and mixing to the flow in a way that most flow particles have an ability to contact the tube wall or flowing near it continuously, where, as Reynolds number increases, the flow swirling increases, and circulation of fluid happens from inner tube surface to center of tube which causes increasing in heat transfer rate. The percentage increase in average Nusselt number for flow in plain tube inserted with twisted tape is proportional inversely to the inlet flow Reynolds number up to 3000 (302% at Re= 784 to 41% at Re=3000) and proportional directly to the inlet flow Reynolds number above 3000 (41% at Re= 3000 to 132% at Re=7000), as shown in **Fig 8.** Therefore the overall enhancement ratio is decreased from 3% to 0.98% for Re 784 to 3000 respectively and then going in increasing to 1.72% for Re=7000 as clear in **Fig 9**.

Comparison of the average Nusselt number computed from this work and **Yang, et al. 2016,** is done for Reynolds number 3000 to 7000. The reason of choosing **Yang, et al., 2016**, work to make comparison with it is because of the same Reynolds number range and twisted tape configuration. As shown in **Fig. 10,** the behavior of the average Nusselt number increase with the Reynolds number is the same for the two works where the Nusselt number curve of this work is above the curve of, **Yang, et al., 2016**, in percentage of 216% to 297% for Reynolds number 3000 to 7000 respectively as shown in **Fig. 11**. The reason of this difference was related to different twisted ratio (y = 2.5 for **Yang, et al.**, **2016** and y = 8.8 for this work) and type of fluid. Also comparison of average 4f computed from this work and **Yang, et al., 2016,** is done as shown in **Fig. 12,** where the percentage difference of 4f are from 31% to 21% for Re= 3000 to 7000 respectively.

4. CONCLUSIONS

The conclusions that are predicted from studying the effect of twisted tape inserted inside plain tube where the tube wall is kept at constant temperature 370K and fluid inside it is crude oil API 28 which enters at 313K are:

1- Significant effect of twisted tape insert inside plain tube, on the heat transfer enhancement from tube surface, is at low flow Reynolds number.
2- The overall enhancement ratio proportional inversely with flow Reynolds number up to 3000 and then proportional directly above Reynolds number 3000.
3- $v^2 - f$ turbulence model is accurate and suitable model for simulation turbulent flow inside circular empty plain tube.
4- *k-ε* turbulence model is more accurate than $v^2 - f$ model for simulated swirling flow inside tube, and the reason of that related to that the *k-ε* model equation contain swirling flow parameter.

5- The static pressure difference between inlet and outlet boundary for plain tube inserted with twisted tape are higher than static pressure difference for empty plain tube.
6- The behavior of average Nusselt number of flow inside tube inserted with twisted tube is increasing continuously in straightway as Reynolds number increase.
7- Avoiding flow Reynolds number 2000 inside plain empty tube because it is leading to low heat transfer performance.

REFERENCES

- ANSYS Fluent 12.1, 2012, "Using flow boundary conditions.
- ANSYS Fluent, 2013, " $v^2 - f$ Turbulence model manual".
- ANSYS Fluent, 2014, "Theory guide".
- Bas, H., and Ozceyhan, V., 2012, "Heat Transfer Enhancement in a Tube With Twisted Tape Inserts Placed Separately From the Tube Wall," Exp. Therm. Fluid Sci., 41, pp. 51–58.
- Bharadwaj, P., Khondge, A. D., and Date, A. W., 2009, "Heat Transfer and Pressure Drop in a Spirally Grooved Tube with Twisted Tape Insert," Int. J. Heat Mass Transfer, 52(7–8), pp. 1938–1944.
- Eiamsa-ard, S., and Promvonge, P., 2010, "Performance Assessment in a Heat Exchanger Tube with Alternate Clockwise and Counter-Clockwise Twisted- Tape Inserts," Int. J. Heat Mass Transfer, 53(7–8), pp. 1364–1372.
- Eiamsa-ard, S., Thianpong, C., and Promvonge, P., 2006, "Experimental Inves- tigation of Heat Transfer and Flow Friction in a Circular Tube Fitted with Regularly Spaced Twisted Tape Elements," Int. Commun. Heat Mass Transfer, 33(10), pp. 1225–1233.
- Giniyatullin, A., and Tarasevich, S., 2013, "CFD Modelling of Subcooled Boil- ing in Tubes with Twisted Tape Insert," ASME Paper No. FEDSM2013- 16298. Lin, Z.-M., and Wang, L.-B., 2009, "Convective Heat Transfer Enhancement in a Circular Tube Using Twisted Tape," ASME J. Heat Transfer, 131(8), p. 081901.
- Gunes, S., Erdemir, D., Ozceyhan, V., and Altuntop, N., 2012, "Numerical Investigation of Thermal Performance of a Tube Fitted With Regularly Spaced Twisted Tape Elements," ASME Paper No. HT2012-58078.
- Kumar Saha, S., and Kumar Pai, P., 2014, "Experimental Investigation of Laminar Flow of Viscous Oil Through a Circular Tube Having Integral Spiral Corrugation Roughness and Fitted With Twisted Tapes With Oblique Teeth," Exp. Therm. Fluid Sci., 57, pp. 301–309.
- Murugesan, P., Mayilsamy, K., Suresh, S., and Srinivasan, P. S. S., 2011, "Heat Transfer and Pressure Drop Characteristics in a Circular Tube Fitted With and Without V-Cut Twisted Tape Insert," Int. Commun. Heat Mass Transfer, 38(3), pp. 329–334.
- Naga Sarada, S., Sita Rama Raju, A. V., Kalyani Radha, K., and Shyam Sunder, L., 2010, "Enhancement of Heat Transfer Using Varying Width Twisted Tape Inserts," Int. J. Eng. Sci. Technol., 2(6), pp. 107–118.
- Ramakumar B. V. N., Arsha J. D., Tayal P., 2016, "Tapered Twisted Tape Inserts for Enhanced Heat Transfer" Journal of Heat Transfer, Vol. 138.
- Thianpong, C., Eiamsa-ard, P., Promvonge, P., and Eiamsa-ard, S., 2011, "Effect of Perforated Twisted-Tapes with Parallel Wings on Heat Transfer Enhancement in a Heat Exchanger Tube," Energy Procedia, 14, pp. 1117–1123.

- Woei Chang, S., Jena Jan, Y., and Shuen Liou, J., 2007, "Turbulent Heat Trans- fer and Pressure Drop in Tube Fitted with Serrated Twisted Tape," Int. J. Therm. Sci., 46(5), pp. 506–518.
- Woei Chang, S., Lirng Yang, T., and Shuen Liou, J., 2007, "Heat Transfer and Pressure Drop in Tube with Broken Twisted Tape Insert," Exp. Therm. Fluid Sci., 32(2), pp. 489–501.
- Yang, L., Han, H., Li, Y. and Li, X., 2016, "A Numerical Study of the Flow and Heat Transfer Characteristics of Outward Convex Corrugated Tubes with Twisted-Tape Insert," Journal of Heat Transfer, Vol. 138.

NOMENCLATURE

A= convection heat transfer area (m^2)

C_1, C_2, C_μ , α , $C_{\varepsilon 1}$, $C_{\varepsilon 2}$, C_L, σ_k, σ_L, $C_1\varepsilon$, $C_2\varepsilon$ = constants of turbulence model

D= inner diameter of test section (m)

D_h= hydraulic diameter (m)

f = elliptic relaxation function

f= friction factor obtained using tape inserts

f_p= friction factor for plain tube

h= convection heat transfer coefficient ($W/m^2.K$)

I= turbulence intensity

k= turbulent kinetic energy (J/kg)

K= thermal conductivity (W/m.K)

L= length of test section (m)

p= static pressure (Pa)

P= pitch (m)

q= heat flux (W/m^2)

Q= total heat transfer (W)

T= temperature (K)

T_b= bulk temperature (K)

T_i= inlet temperature (K)

T_o= outlet temperature (K)

T_s= average surface temperature tube wall (K)

U= fluid velocity through test section (m/s)

u= velocity vector (m/s)

u, v, w= mean velocity components (m/s)

x= distance along tube (m)

x_i, x_j, x_k= cartesian coordinates (m)

Δp= pressure drop across the test section (Pa)

Greek symbols

ε = dissipation rate of k (W/kg)

η= overall enhancement ration

μ= viscosity (Pa.s)

ρ= density (kg/m³)

Non-dimensional Groups

Nu, Nu_p= Nusselt number with tape inserts and for plain tube

Re= Reynolds number

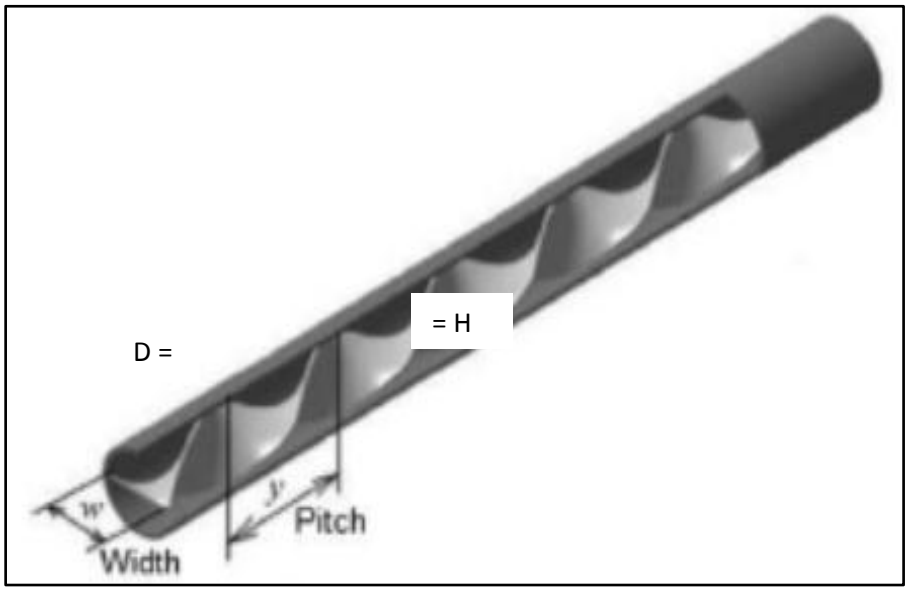

Figure 1. 3D view of tube inserted with twisted tape.

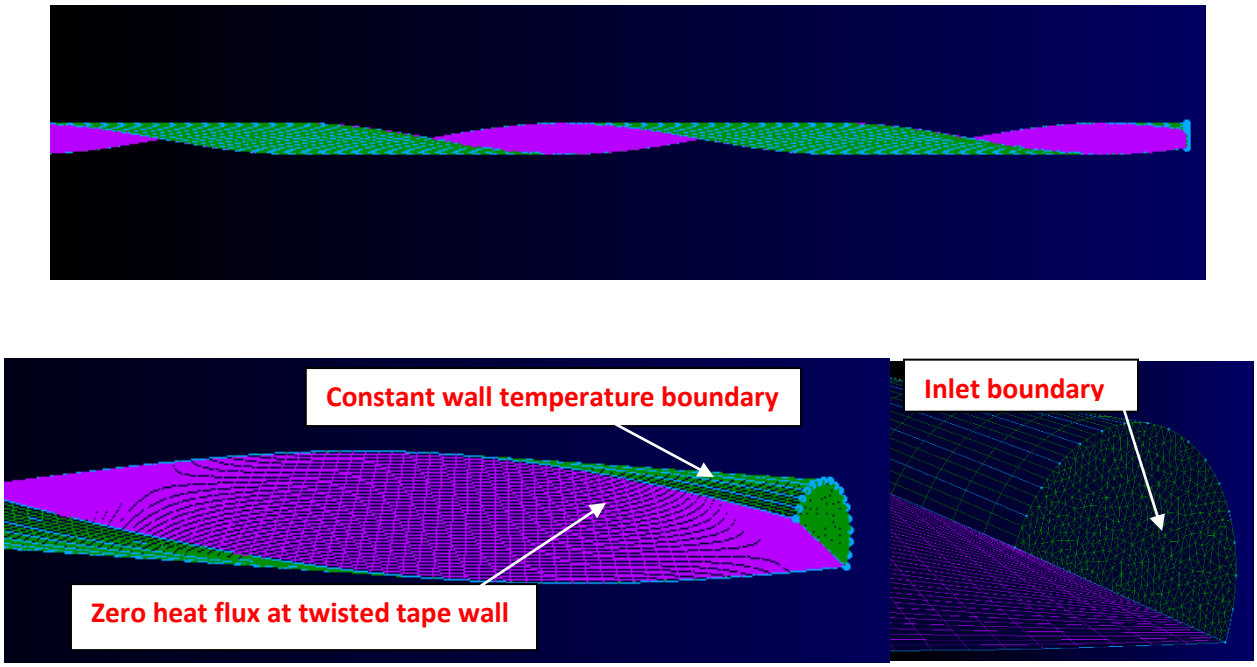

Figure 2. (a) Hybrid mesh of plain tube inserted with twisted tape.

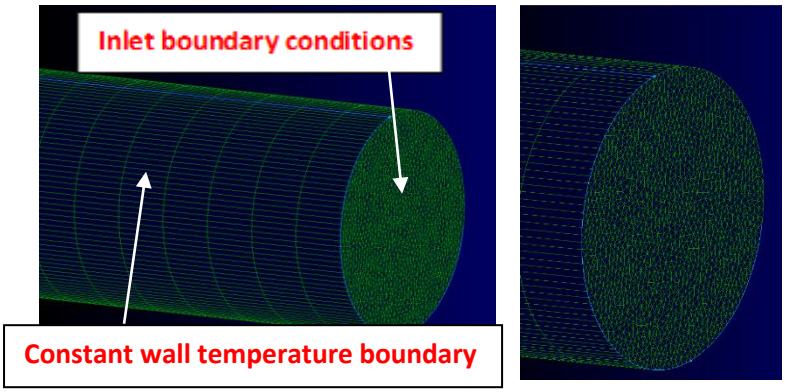

Figure 2. (b) Hybrid mesh of plain empty tube.

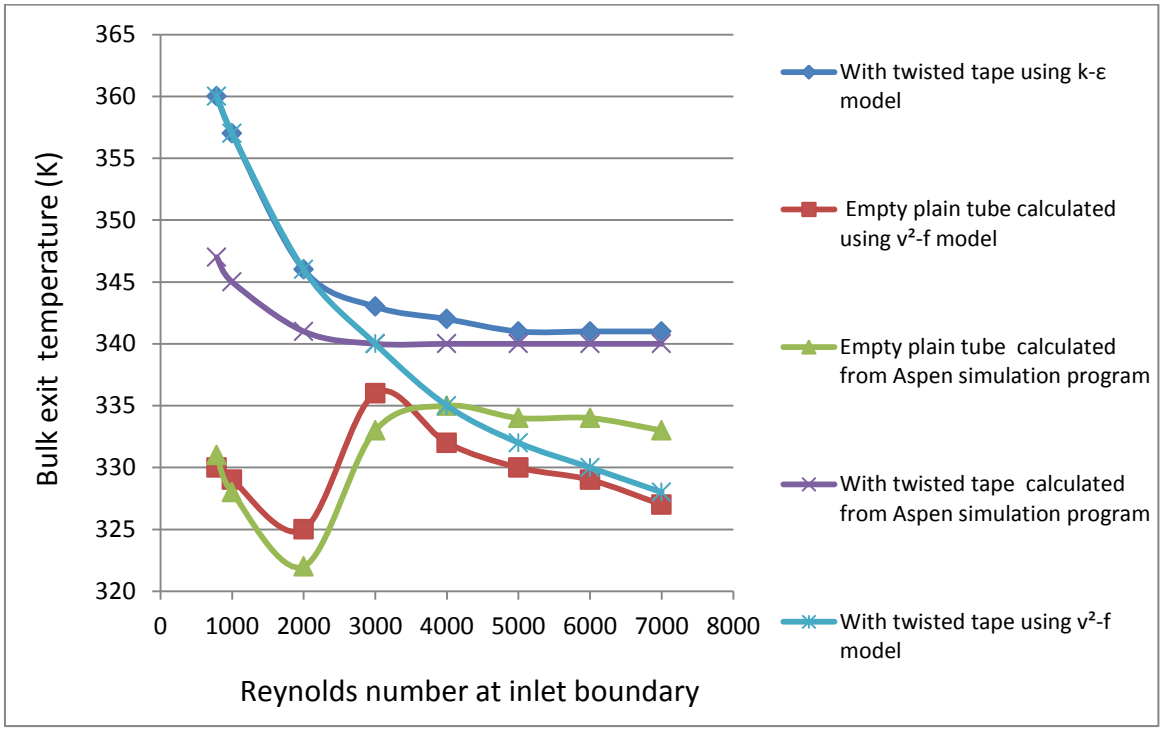

Figure 3. Bulk exit temperature of crude oil API 28 from empty plain tube and plain tube with inserted with twisted tape.

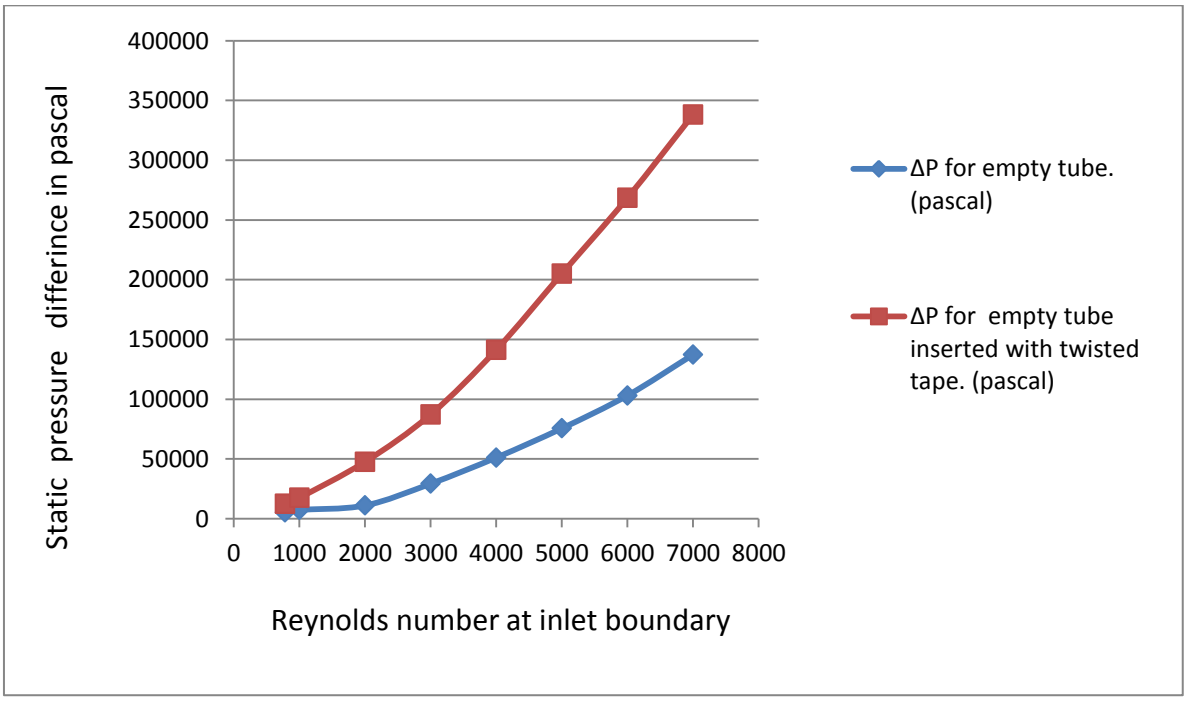

Figure 4. Variation of static pressure difference with inlet Reynolds numbers for empty plain tube and plain tube inserted with twisted tape by using ANSYS Fluent.

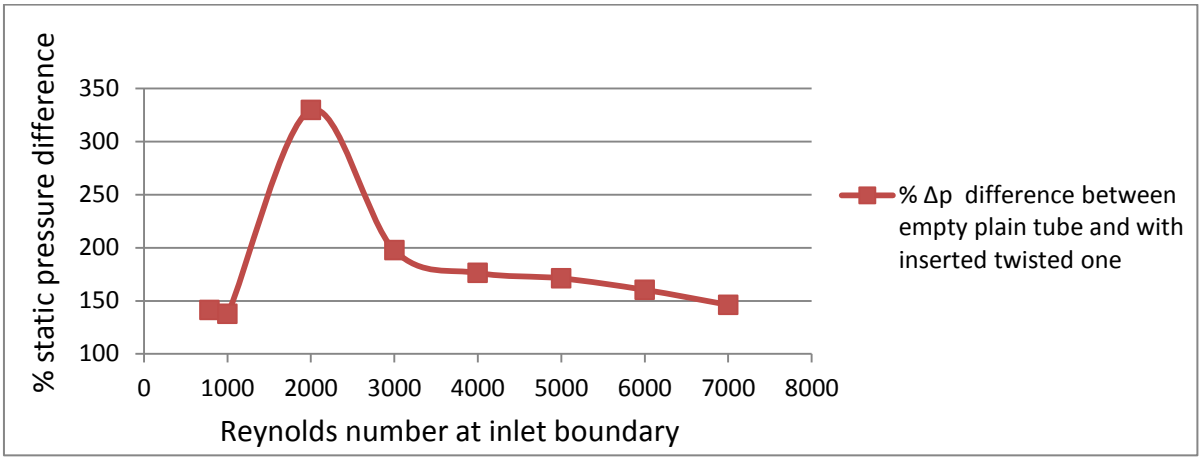

Figure 5. Variation of percentage static pressure difference increase with inlet Reynolds numbers for plain tube inserted with twisted tape over empty plain tube.

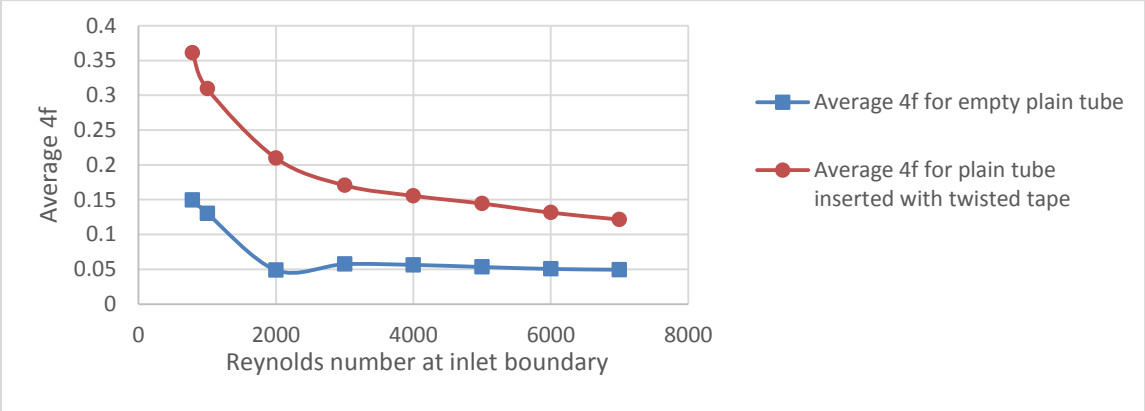

Figure 6. Variation of average tube surface friction factor with inlet Reynolds numbers for empty plain tube and plain tube inserted with twisted tape.

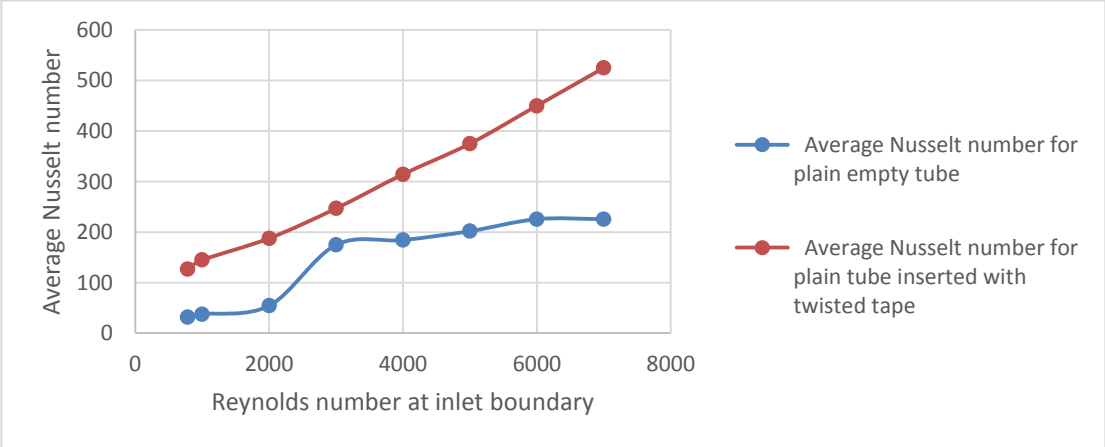

Figure 7. Variation of average tube surface Nusselt number with inlet Reynolds numbers for empty plain tube and plain tube inserted with twisted tape.

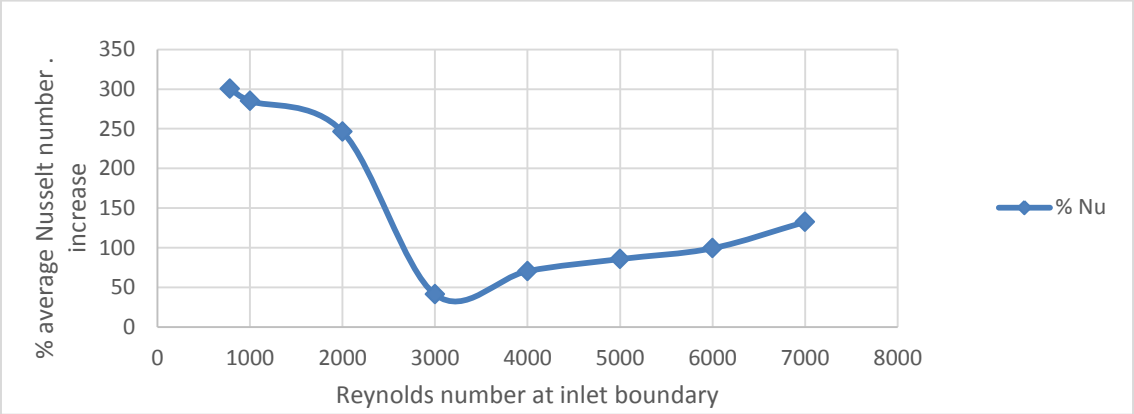

Figure 8. Variation of percentage increase of average Nusselt number with inlet Reynolds numbers for plain tube inserted with twisted tape over empty plain tube.

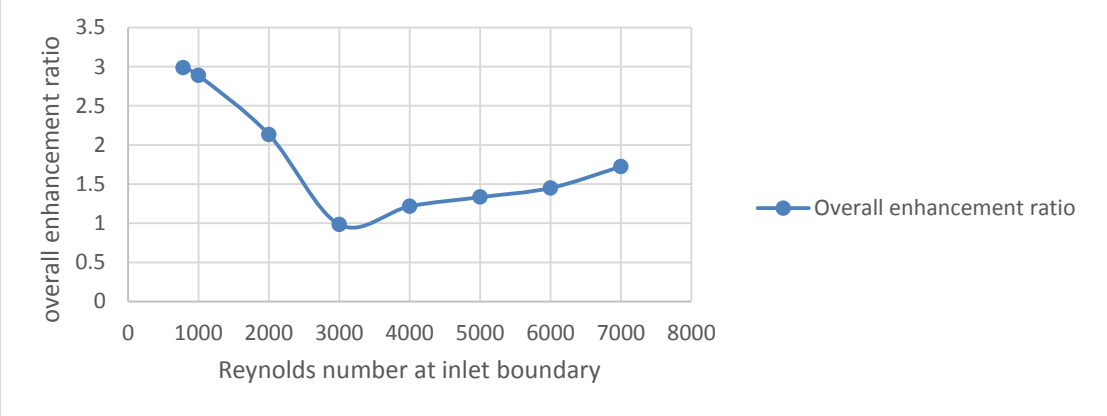

Figure 9. Variation of overall enhancement ratio with inlet Reynolds numbers for empty plain tube and plain tube inserted with twisted tape.

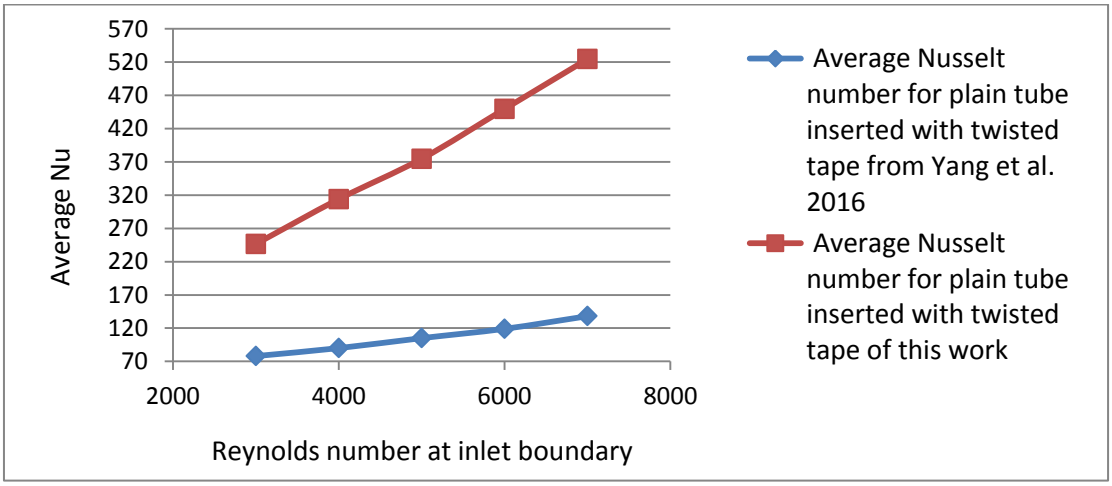

Figure 10. Comparison of average Nusselt number computed from this work and Yang et al. 2016.

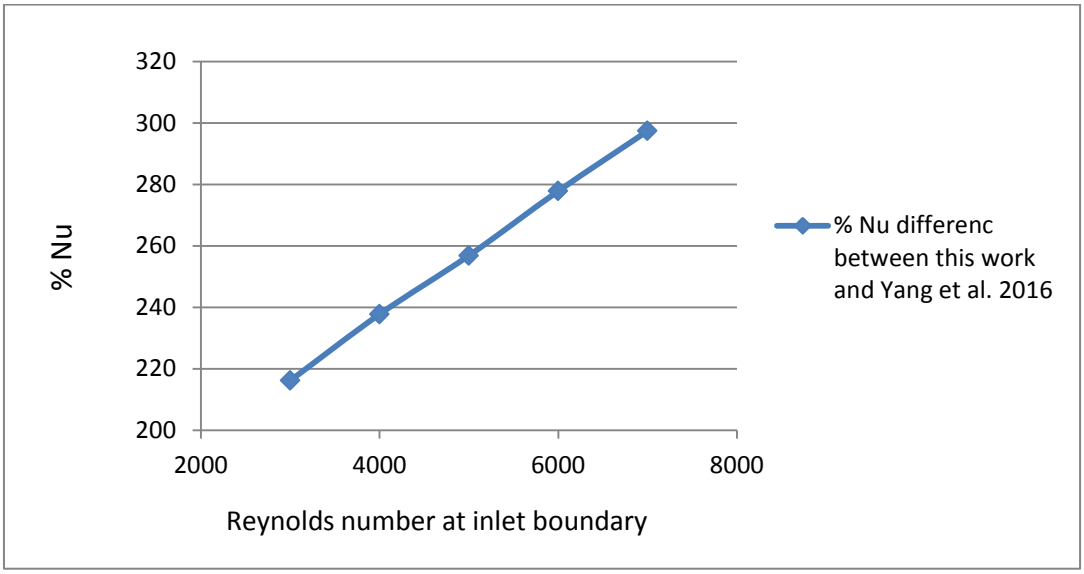

Figure 11. Percentage average Nusselt number differences with Reynolds number between this work and **Yang, et al., 2016 work.**

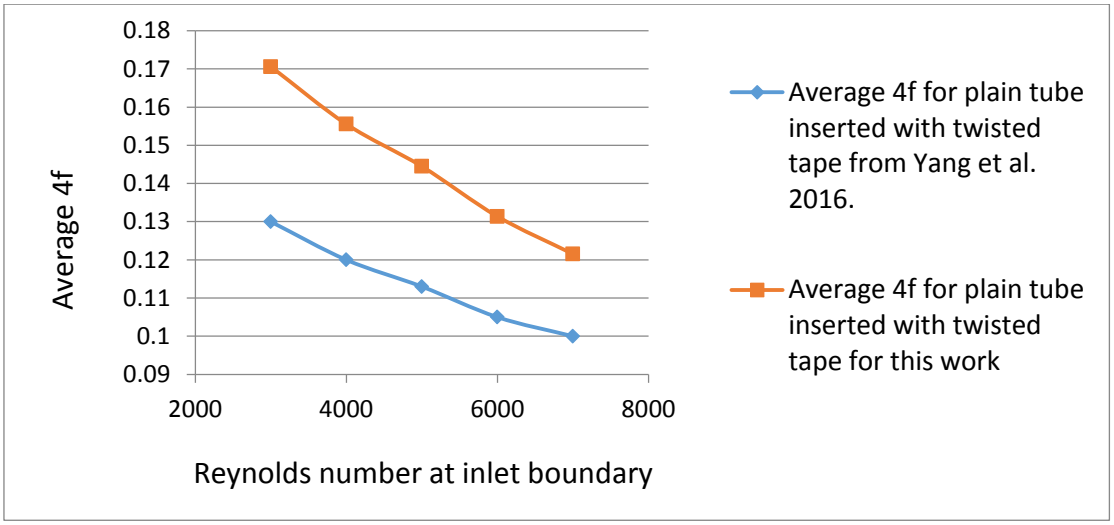

Figure 12. Comparison of average 4f computed from this work and **Yang, et al., 2016**.